ISSN- 2350-0530(O), ISSN- 2394-3629(P)
Index Copernicus Value (ICV 2018): 86.20
DOI: 10.5281/zenodo.3698202

INTERNATIONAL JOURNAL OF RESEARCH – GRANTHAALAYAH
A knowledge Repository

Science

THEORETICAL STUDY OF THE POTENTIAL ANTI-CHAGASIC PHARMACOLOGICAL TOOL MACHILIN G: A STUDY OF MOLECULAR DOCKING

Victor da Silva de Almeida [1], Victor Moreira de Oliveira [1], Carlos Lacerda de Morais Filho [1], Francisco Rogênio da Silva Mendes [1, 2], Aluísio Marques da Fonseca [3], Emmanuel Silva Marinho [*1]

[*1] Chemistry Department/FAFIDAM, State University of Ceará-Brazil
[2] Northeast Biotechnology Network / RENORBIO, State University of Ceará–Brazil
[3] Academic Master'sDegree in Sociobiodiversity and Sustainable Technologies, Universidade da Integração Internacional e da Lusofonia Afro-Brasileira,-Brazil

Abstract

Chagas disease caused by Trypanosoma cruzi, which affects thousands of people around the world. In recent years, research aimed at the discovery of new drugs has started to seek specific macromolecular targets for the disease. In this context, enzymes are therapeutic targets of great interest, since they play a fundamental role in many diseases. In this context, the present work aimed to characterize the Machilin G molecule conformationally and evaluate its interactions in the main therapeutic targets involved in the replication of T. cruzi. To understand the inhibitory mechanism of Machilin G on the evolutionary forms of T. cruzi, the molecule it was conformationally characterized, until reaching thermodynamic stability, and then it was submitted to molecule docking routines, having as protein targets the Cruzain enzymes, Tripanothione reductase and glyceraldehyde-3-phosphate dehydrogenase (TcGAPDH). Machilin G had its structure optimized using semi-empirical quantum calculations, through this technique it was possible to generate the thermodynamically more stable conformation. Through the method of analysis of the computer simulations of molecular anchoring, it was demonstrated that the ligand Machilin G was coupled to the active site of the enzyme TcGAPDH, at distances close to the chalepin. In relation to Cruzain, it is possible to highlight that the ligand Machilin G does not interact with the amino acids of the active site of the enzyme, being at a considerable distance in relation to the ligand KB2. Regarding the enzyme Trypanothione reductase, the ligand Machilin G had few interactions with the amino acids of the active site. The intermolecular interactions found for the complex formed and the values obtained at a distance from the enzyme residues indicate that Machilin G has potential application as a new inhibitor of the enzyme Trypanosoma cruzi TcGAPDH. The present work being a fundamental step for the understanding of Machilin G mechanism of action in view of the evolutionary forms of the t-cruzi parasite.

Keywords: Cruzain; Docking Molecular; Frontier Orbitals; Glyceraldehyde-3-Phosphate Dehydrogenase; Tripanothione Reductase.

ISSN- 2350-0530(O), ISSN- 2394-3629(P)
Index Copernicus Value (ICV 2018): 86.20
DOI: 10.5281/zenodo.3698202

Cite This Article: Victor da Silva de Almeida, Victor Moreira de Oliveira, Carlos Lacerda de Morais Filho, Francisco Rogênio da Silva Mendes, Aluísio Marques da Fonseca, and Emmanuel Silva Marinho. (2020). "THEORETICAL STUDY OF THE POTENTIAL ANTI-CHAGASIC PHARMACOLOGICAL TOOL MACHILIN G: A STUDY OF MOLECULAR DOCKING." *International Journal of Research - Granthaalayah*, 8(2), 188-211. https://doi.org/10.5281/zenodo.3698202.

1. Introduction

Originally arising in rural areas of the Americas in the 20th century, Chagas disease caused by *Trypanosoma cruzi*, known as American trypanosomiasis, is a parasitic disease that affects thousands of people worldwide and is a neglected disease in the Americas (mainly in rural areas of Latin America , where poverty is widespread, however, in large numbers in urban areas, where about 60% of people are infected). Chagas disease is caused by infection by the protozoan parasite Trypanosoma cruzi (Tc) [1][2]. Due to increasing urbanization this disease has changed its progressive epidemiological pattern and has spread to other continents, becoming a public health problem, current estimates indicate that about 7 million people are infected with *Trypanosoma cruzi* worldwide, and mainly in the countries of continental Latin America, causing an additional 7000 deaths per year and exposing the risk of infection to more than 25 million people[3][4]. these data become more worrying, due to the loss of efficiency of benznidazole, the only drug currently recommended for the treatment of the disease, and which is associated with serious side effects. Therefore, it is necessary to identify new pharmacological targets for the selection of molecules with good efficacy against the parasite and low toxicity[5]. To combat this disease, several chemical therapeutic methods are tested in order to discover the most effective way to reduce the damage that *Trypanosoma cruzi* brings to health. The form of transmission to humans is mainly through the feces of triatomine insects, known in Brazil as "barbers", for the habit of stinging the faces of their victims. In recent years, research aimed at the discovery of new drugs has started to seek specific macromolecular targets for the disease. In this context, enzymes are crucial for the evolution of parasitic forms. Currently, the *Cruzain* enzymes, Tripanotiona reductase and Trypanosoma cruzi glyceraldehyde-3-phosphate dehydrogenase (*TcGAPDH*), are the main enzymes studied with targets and are therapeutic targets of great interest, since they play a fundamental role in many diseases[6]. In this search for potential pharmacological tools Machilin G showed antitrypanosomal activity, with an inhibitory concentration (IC50) of 2.2 μM and potential antileishmanial activity, with a value of 50.54 μM, against *L. donovani*, indicating that it is a molecule that has potential for the development of antichagasic drugs[7][8][9].

Molecular modeling techniques have been promoting the understanding of the mechanisms of action of drugs, making it possible to characterize the molecules conformationally[10][11][12], as well as simulating the fit between the molecule and its potential therapeutic target (molecular docking)[13][14]. For the study of new compounds and their possible activities biological, it is essential to know the structure of the molecule in question, defining its thermodynamically more stable conformation, characterizing the surface behavior of the potential, identifying the possible electrophilic and nucleophilic sites[15][16]. In this context, molecular modeling uses *in silico* methods and theoretical calculations, which allow the characterization of molecular structures and their properties, in addition to predicting the mechanism of interaction between molecules and possible biological targets[14], [17][18] .In this context, the present work aimed to characterize

ISSN- 2350-0530(O), ISSN- 2394-3629(P)
Index Copernicus Value (ICV 2018): 86.20
DOI: 10.5281/zenodo.3698202

the Machilin G molecule conformationally, and to evaluate its interactions in the main therapeutic targets involved in the replication of T-cruzi. The present work being a fundamental step for the understanding of Machilin G mechanism of action in view of the evolutionary forms of the *T-cruzi* parasite.

2. Materials and Methods

2.1. Obtaining Protein Structures and Atomic Coordinates

The protein structures studied in this work were obtained from RCSB protein da bank (https://www.rcsb.org/)[19] and the two-dimensional coordinates of the ligand in the PubChem repository[20], is an open chemistry database at the National Institutes of Health (https: //pubchem.ncbi.nlm.nih.gov/compound/Machilin-G).

2.2. Structural Optimization

The study of the Machiling G molecule was carried out using the quantum method at the semi-empirical level Parametric Method 3 (PM3)[21], an algorithm that shows excellent correlation with experimental results and requires less computational resources than the traditional Ab initio method. For structural optimization and electronic characterization of the Machilin G molecule, it was performed using the semi-empirical quantum method Parametric Method 3 (PM3)[22], an algorithm that shows excellent correlation with experimental results and requires less computational resources than the traditional Ab initio method. The ArgusLab (tm) Version 4.0 software was used to support the execution of the PM3 code, configured so that the Hartree-Fock SCF performs 200 interactions with 10-10 kcal / mol closed-shell convergence[23].Using the data generated from the optimization (file.out), it was possible to calculate the single point and determine the structural, electronic and reactivity properties. With the electronic characterization data it was possible to plot the potential surface map, and with the reactivity data to plot the Frontier orbitals[24].

2.3. Enzyme Preparation

The three-dimensional structures of the proteins *Cruzain, Tripanotiona Redutase* and *TcGAPDH* were obtained from the protein data bank database https://www.rcsb.org/structure/3iut, https://www.rcsb.org/structure/1k3t and https: //www.rcsb.org/structure/1gxf, *Cruzain* classified as protein hydrolase a structure crystallized in the complex with an inhibitor of tetrafluorophenoxymethyl ketone organism type *Trypanosoma cruzi* expression system type *komagataella pastoris mutation* (s): 2, method: x-ray diffraction, resolution: 1.2 å, r-value free: 0.153, r-value work: 0.127, deposited as 3iut[25]. The *TcGAPDH* protein structure of glycosomal *glyceraldehyde-3-phosphate dehydrogenase* from *Trypanosoma cruzi* complexed with *Chalepin*, the coumarin derivative inhibitor classified as oxidoreductase, organism (s): *trypanosoma cruzi*, expression system: escherichia coli experimental data snapshot method: x-ray diffraction resolution : 1.95 å r-value free: 0.280 r-value work: 0.201 deposited as 1k3t[26]. *Trypanothione reductase* in complex with quinacrine mustard inhibitor classification: oxidoreductase organism (s): *Trypanosoma cruzi* expression system: *escherichia coli* experimental data snapshot method: x-ray diffraction resolution: 2.7 å, r-value free: 0.250, r-value work: 0.190, deposited as 1gxf[27].

ISSN- 2350-0530(O), ISSN- 2394-3629(P)
Index Copernicus Value (ICV 2018): 86.20
DOI: 10.5281/zenodo.3698202

All water molecules were removed from protein structures, reducing interference with the binding of Machilin G to the target enzyme. Polar hydrogen atoms missing from the structure were added using AutoDock Tools. After that, the docking was carried out with each protein with residues using the Machilin G ligand as a comparison, and each open protein with residues had its specific ligand to be compared with the Machilin G (Cruzain-kb2) ligand (TcGAPDH-chapelin BRZ) (Trypanothione reductase-quinacrine mustard QUM) in order to find the best result in the active site of the molecule, After choosing the best result saved the protein pdb and the ligand with the best rmsd and affinity, then each protein was opened without residues and with the best Docking was done between the amino acid residues and the protein and its respective ligand. And then with the help of Discovery, you can visualize the types of interactions formed[28].

2.4. Molecular Docking

Molecular attachment of the ligand to receptor was performed using 4-way multithreading and the AutoDock Tools (version 1.5.7) [29]graphical interface that runs AutoDock Vina (version 1.1.2)[30]. to carry out molecular docking, some protocols were used, such as delimiting the grid box of each protein, *Cruzain* protocol (pdb: 3iut) grid box center_x = 6,612, center_y = -0.436, center_z = 8,052, size_x = 116, size_y = 106, size_z = 126, spacing = 0.431 and exhaustiveness = 8. *TcGAPDH* protocol (pdb: 1k3t) grid box center_x = 19.822, center_y = 0.455, center_z = 24.804, size_x = 116, size_y = 112, size_z = 122, spacing = 0.931 and exhaustiveness = 8. *Trypanothione reductase* protocol (pdb: 1gxf) grid box center_x = 44.196, center_y = 3.102, center_z = -0.054, size_x = 126, size_y = 90, size_z = 126, spacing = 0.775 and exhaustiveness = 8.The images of the two-dimensional graphs of the interactions and three-dimensional visualization of the complex formed were generated using the Discovery Studio visualizer® [31]and UCSF Chimera [[32]

3. Results and Discussions

The advances in information technologies have provided an increase in access to data, allowing quick access to structural and physical-chemical characteristics of several molecules. These repositories provide an incentive in the study of the characterization of several molecules, since they provide structural descriptors, which serve as initial inputs for further studies. In this perspective, the online virtual repository PubChem® [20]was used to obtain initial information about Machilin G acetate (PubChem CID: 10450921), as its official nomenclature by IUPAC (5 - [(2S, 3S, 4R, 5R) -5- (3,4-dimethoxyphenyl) -3,4-dimethyloxolan-2-yl] -1,3-benzodioxole), molecular formula (C21H24O5), molecular weight (356.4 g / mol), exact mass (356.162374 g / mol), XLogP3-AA (4.3), monoisotopic mass (356.162374 g / mol), polar topological surface area (46.2 $Å^2$). The two-dimensional coordinates show in their structure 5 hydrogen bonding donor atoms, 4 Rotatable Bond Count, and 4 Defined Atom Stereocenter Count and (figure 1).

ISSN- 2350-0530(O), ISSN- 2394-3629(P)
Index Copernicus Value (ICV 2018): 86.20
DOI: 10.5281/zenodo.3698202

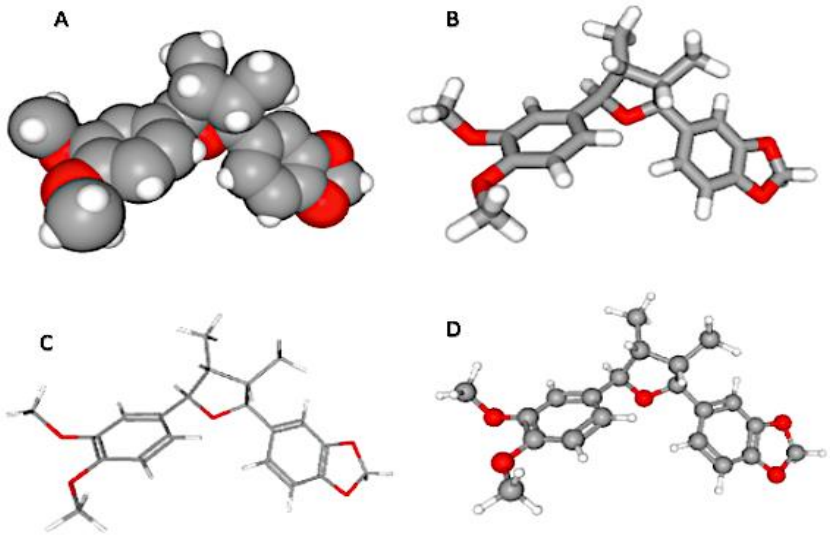

Figure 1: Structural representations of the Machilin G (A) Space-Filling (B) Sticks (C) Wireframe (D) Ball and Stick

3.1. Geometric Optimization and Structural Properties

As atoms do not present uniformity in real cases due to the electronic cloud, Geometry understands the organization between the arrangements of atoms, an important parameter to predict the polarity of a molecule. When a molecule is taken directly from a virtual repository, its conformation is not more stable[12][22][23][33][34]. In this case, the use of molecular modeling is introduced, an important tool to help the understanding of fundamental concepts of structure-activity relationships and mechanism of action of molecules One of the processes used in modeling is the process of geometric optimization, which, using theoretical calculations, seeks to retain each atom in its regions with lower levels of potential energy making the molecule thermodynamically more stable (explain what molecular geometry is)[35][36][37] [34]. The geometrically optimized Machilin G ligand (Figure 2) through semi-empirical quantum calculations, obtaining the structure theoretically close to its native form and energy, it is possible to structurally characterize atomic properties, connections and angles. When analyzing atomic properties, one can notice the presence of variations in the partial charges of atoms of the same nature since the carbon atoms ranged from -0.059 to 0.233, the oxygen atoms from -0.491 to -0.364 and the hydrogens varying from 0.023 to 0.117. In the final geometry of Machilin G after optimization, all the analyzed bonds were characterized by the predominance of covalence, where it can be highlight the bonds (1, 6, 10, 39, 43, and 47) between carbon as second order bonds (Table S1- supplementary material). In addition, the links (21, 22, 24, 27 and 30) between the carbons are known for their rotation (Table S2- supplementary material). Complementing the conformational analysis, the largest and smallest angles between the joints were identified, angles 81 (CCO) and 39 (CCC) with 128.3547 ° and 102.2908 ° respectively; and at greater and lesser torsion angles, systems 123 (CCCH) and 70 (HCCH) with 179.9692 ° and -179.9499 ° respectively (Table S3 and S4- supplementary material).

ISSN- 2350-0530(O), ISSN- 2394-3629(P)
Index Copernicus Value (ICV 2018): 86.20
DOI: 10.5281/zenodo.3698202

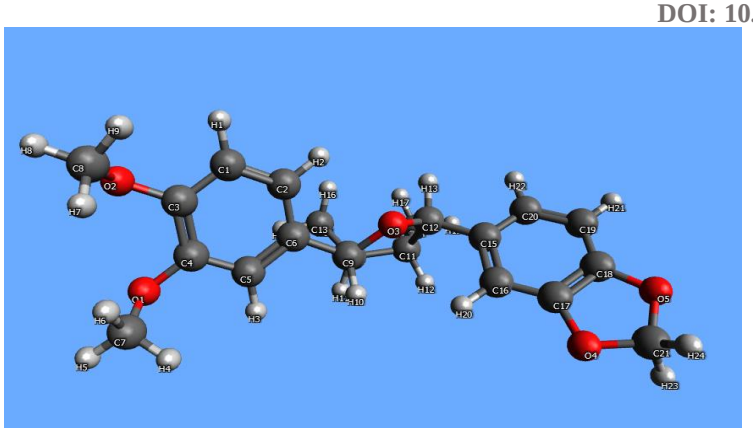

Figure 2: Optimized three-dimensional structure of the Machilin G

3.2. Frontier Orbitals

A category of chemical-quantum descriptors widely used in studies is related to the energy of the HOMO and LUMO frontier orbitals[37]. The HOMO is an orbital occupied with greater energy, it is linked to the ionization potential, and the electron-donating capacity of the molecule, the LUMO and showing the region where it has the highest electron density, LUMO is the unoccupied orbital with the lowest energy, is related to electronic affinity and with the ionization potential and electron-acceptor capacity of the compound, showing the lowest electronic density of the molecule. From these definitions, two important characteristics can be observed: the greater the energy of HOMO, the greater the electron-donor capacity and, the lower the energy of LUMO, the lower the resistance to accept electrons. The variation between the orbital limit values, called GAP, indicates the energy required for an electron to transition[34][38][39]. The greater the value of the difference, the lower the molecular reactivity and the greater the molecular capacity. Machilin G presented the energy value -0.331477 eV for the HOMO orbital and having atoms C18, C20, C21, C23, O24, O26, H40 AND H50 as contributors, where all showed symmetry between the positive and negative phases (Figure 3 A). The LUMO orbital had an energy value of 0.000739 eV with atoms C1, C2, C3, C4, C5, C6, C18, C19, C20, C21, C22, C23 showing symmetry between the positive and negative phases (Figure 3 B).

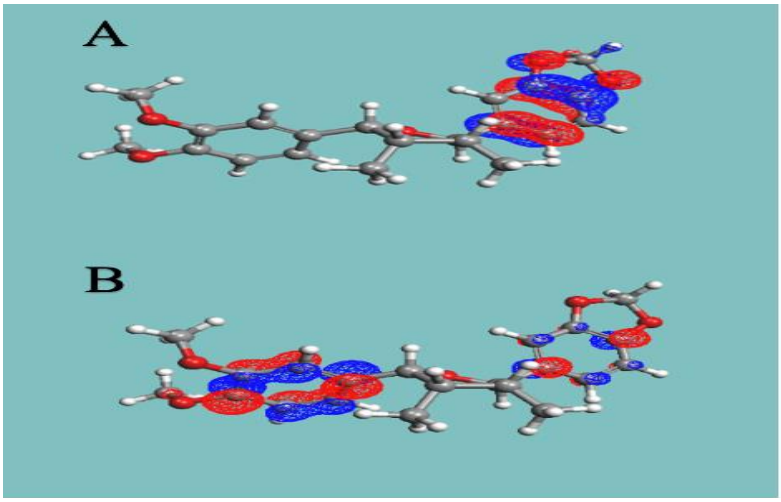

Figure 3: Frontier orbitals of the Machilin G HOMO (A) and LUMO (B)

ISSN- 2350-0530(O), ISSN- 2394-3629(P)
Index Copernicus Value (ICV 2018): 86.20
DOI: 10.5281/zenodo.3698202

3.3. Mulliken Population Analysis

Mulliken atomic charges (Mulliken population analysis) and surface map of electrostatic potential Mulliken population analysis divides the charge densities between the atoms, regardless of electronegativity[40]. the same nature are notorious, where carbon atoms range from -0.3216 to 0.0620, in oxygen -0.2564 to -0.1941 and hydrogen atoms from 0.0879 to 0.2173[41][42]. The visualization and analysis of charges is possible through the surface map of potential electrostatics, as it allows to characterize electrophilic and nucleophilic regions, showing how complex molecules interact[43][44][45]. Through the MESP of Machilin G it was possible to perceive defined regions, since the regions in red signify regions with a high concentration of collections and the regions in white have a low concentration of charge. The regions highlighted in red are due to the presence of an oxygen atom, since they are more electronegative atoms than carbons and hydrogens (Figure 4)

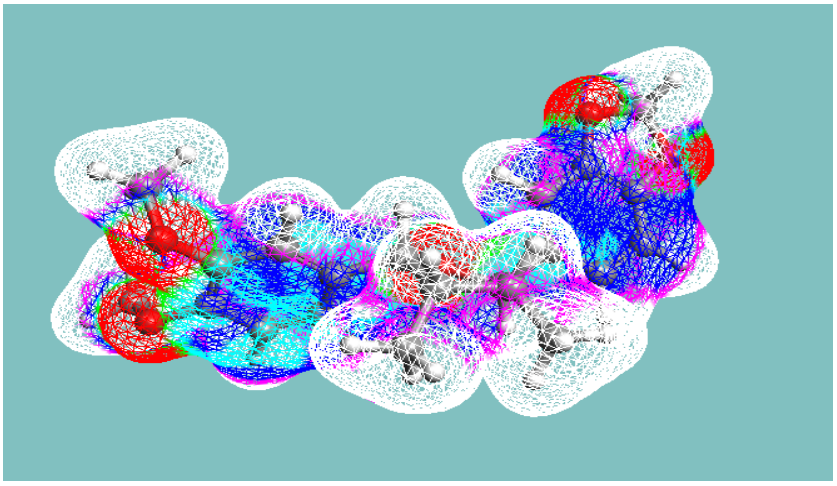

Figure 4: Machilin G electrostatic potential surface map (MESP)

3.4. Molecular Docking

The computational technique of molecular docking is one of the methods used in the therapeutic study of drugs where tests are carried out on possible bioactive molecules (ligands) for a given molecular target, the molecule can assume certain orientations of molecular fitting within the ligand site of the target, these processes involve energy such as the enthalpic (maximum energy of a system) and the entropic (thermodynamic energy related to chemical reactions)[17][34][46], through this it can be said that the molecular structure that presents less amount of energy necessary to bind to the active site, it will be the one that, theoretically, will perform the best result of biological activity. Through these coupling techniques, it was possible to discover new drugs that are increasingly improved, causing less damage to health[47][48].

The docking routines were performed with Machilin G and benznidazole (control), in which the simulations were classified based on the free binding energy [49]and the conformations that presented RMSD up to 2.0 Å [50]Variations in the RMSD values from 0.907 to 1.653 Å and affinity energies were observed from -7.8 to -5.1 kcal / mol (Table 1) staying within the standards considered with valid positions for molecular docking.

ISSN- 2350-0530(O), ISSN- 2394-3629(P)
Index Copernicus Value (ICV 2018): 86.20
DOI: 10.5281/zenodo.3698202

Table 1: RMSD and affinity energy values calculated in molecular docking simulations

Enzyme	**Ligand**	**RMSD (Å)**	**Affinity (kcal/mol)**
Cruzain	Benznidazole	1.653	-5.1
Cruzain	Machilin G	1.206	-6.9
TcGAPDH	Benznidazole	1.876	-5.5
TcGAPDH	Machilin G	0.907	-7.8
Tripanotiona Redutase	Benznidazole	1.514	-5.3
Tripanotiona Redutase	Machilin G	1.507	-7.6

3.5. Analysis of Molecular Docking Simulations Between *Cruzain* And Machilin G

The enzyme *Cruzain*, a fundamental cysteine protease of *T. cruzi*, is a validated therapeutic molecular target for Chagas disease[25]. It is present during all stages of the parasite's evolutionary cycle and is essential for its nutrition and development. Belonging to the papain family in which it catalyzes hydrolysis reactions of peptide bonds. More specifically, it is responsible for the degradation of host cell proteins and, therefore, contributing to the infection process. Its crystallographic structure is composed of a polypeptide arrangement of 215 amino acids, folded into two domains, where one is predominantly α-helix (C-terminal) and the other consists of extensive interactions of antiparallel (N-terminal) β-leaves. For enzymes of the papain family, there is an extensive gap between the two domains, where the catalytic site composed of the residues Cys25, His159 and Asn175, which form the so-called catalytic triad, is located[25]. The catalytic site has four binding subsites, determined as S1, S2, S3 and S1 '. The main one, the S2 subsite, is responsible for the specificity of the enzyme. Little exposed to the solvent, it is bounded by the side chains of hydrophobic residues, Met68, Ala133, Leu67, Leu157 and Gly160, being prone to groups of substances insoluble in water[25]. However, the presence and flexibility of the Glu205 residue at the end of this subsite gives it a negative characteristic, as it also allows interactions with positively charged groups. The S1, S3, and S1 'subsites are less defined and more exposed to the solvent, however they contain amino acid residues that are fundamental for catalytic activity. One of the residues of the catalytic triad, Cys25 is present in the S1 subsite, as well as residues Gln19, Gly23, Ser64 and Leu67 [25][51]. In the S3 sub-site there are the residues Ser61, Gly65, Gly66 and Leu67, while in the S1 'sub-site are the other two residues of the catalytic triad Hys159 and Asn175, together with Asp161 and Trp184. With the Chimera[32] program it is possible to see the types of interactions of the amino acids that are present in the protein and ligand. The first to be done was that of *Cruzain* with the ligand Machilin G, the amino acids to be calculated distances were (Gln-19; Cys -25; Ser-61; Gly-65; Gly-66; Leu-67; Asp161; His162; Asn-182; Trp-184; Glu-208), comparing the distances of the benzonidazole ligands, KB2, Machilin G go that had the shortest distances between the ligand and the amino acid was KB2(Table 2). The ligand Machilin G presented the following interactions two interactions with Arg A: 10 (conventional hydrogen bond), a Phe A: 39 (pi-pi t-shaped) interaction, a Phe A: 39 (pi-alkyl) bond, a bond pro A: 44 (alkyl). Six van der walls interactions (His A: 43; Gly A: 42; Leu A: 40; Trp A: 7; Leu A: 45) (figure 5).

ISSN- 2350-0530(O), ISSN- 2394-3629(P)
Index Copernicus Value (ICV 2018): 86.20
DOI: 10.5281/zenodo.3698202

Table 2: Distances between the *Cruzain* residues and the ligands

Cruzain residue	Benznidazole	KB2	Machiling
Gln19	26.4 Å	3.1 Å	21.2
Cys25	23.8 Å	1.8 Å	21.8
Ser61	33.3 Å	2.8 Å	30.4
Gly65	30.4 Å	3.2 Å	29.4
Gly66	28.3 Å	2.9 Å	28.8
Leu67	25.0 Å	3.9 Å	26.2
Asp161	30.2 Å	3.4 Å	29.4
His162	26.0 Å	3.3 Å	24.0
Asn182	20.3 Å	7.7 Å	17.5
Trp184	26.9 Å	6.3 Å	22.2
Glu208	22.6 Å	4.0 Å	24.2

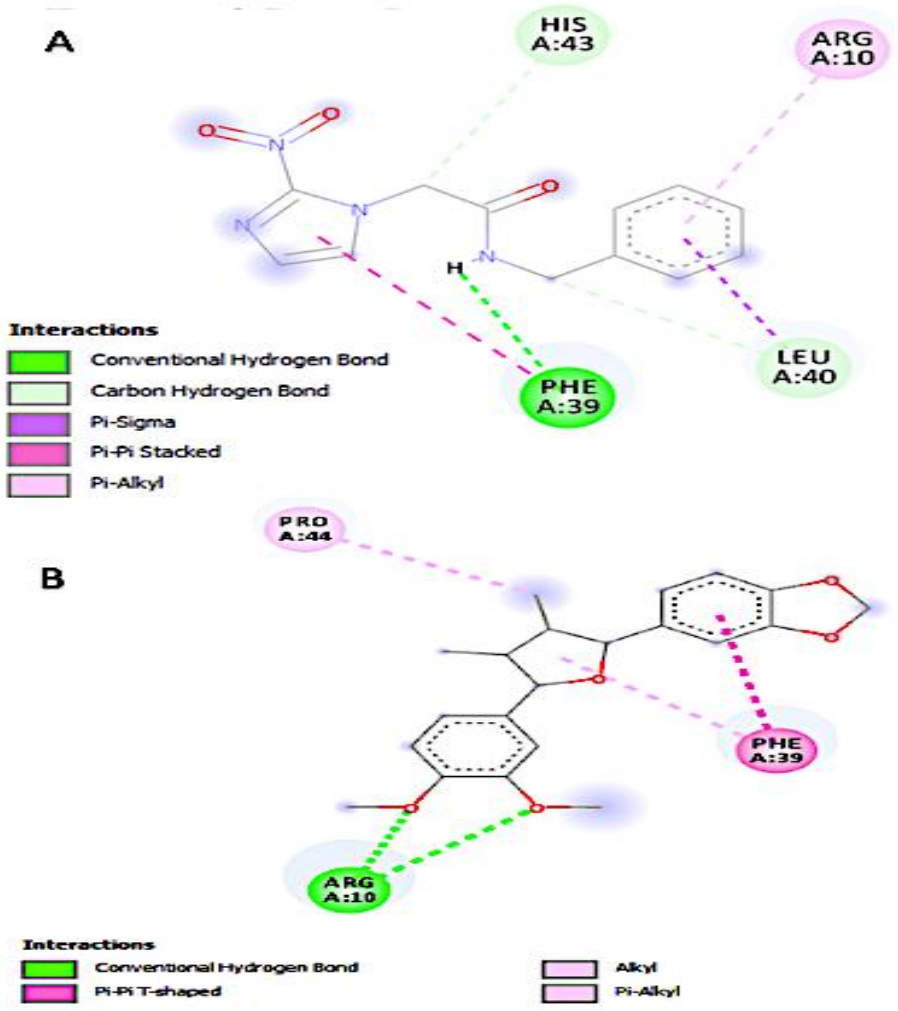

Figure 5: Two-dimensional molecular map for intermolecular interactions between *Cruzain* and Benznidazole (A), Machilin G (B).

ISSN- 2350-0530(O), ISSN- 2394-3629(P)
Index Copernicus Value (ICV 2018): 86.20
DOI: 10.5281/zenodo.3698202

3.6. Analysis of Molecular Docking Simulations Between *Trypanosoma Cruzi Glyceraldehyde-3-Phosphate Dehydrogenase* (*Tcgapdh*) And Machilin G

The enzyme *Trypanosoma cruzi glyceraldehyde-3-phosphate dehydrogenase* (*TcGAPDH*)is characterized by being a tetramer enzyme with subunits of approximately 359 residues, known for being the sixth enzyme to participate in the glycolytic pathway in both humans and trypanosomes, thus catalyzing the conversion of glyceraldehyde-3-phosphate in 1,3-bisphosphoglycerate in the presence of the cofactor NAD + (essential for the biological activity of the enzyme), and inorganic phosphate. In *T. cruzi* the predominant intracellular trypanosomatides depend mainly on glycolysis for the production of ATP, inhibiting *TcGAPDH* would prevent *T. cruzi* from being infectious, this is one of the reasons why this enzyme is exploited as a therapeutic target by research[5] [26] [52][26] . Performing the distances with the *TcGAPDH*, the ligand Machilin G has rmsd 0.907, with an affinity of -7.8, The amino acids that were performed the distances were (Ile13; Pro136; Cys166; Thr167; His194; Thr197; Asp210; Arg249)(Table 3), the types of interactions were 11 van der walls interactions (Pro c: 136, Ser c: 134, Arg c: 12, Ser c: 165, Thr c: 167, Val b: 203, Tyr c: 196, Glu c: 336, Thr c: 197, Ala c: 228, Thr c: 226) four conventional Hydrogen bond (Cys c: 166); (Asn c: 335); (Ala c: 198), a pi-donor pi-sulfur bond (pi- donor hydrogen bond) (Cys C: 166), a pi-sigma bond (His C: 194), a stacked pi-pi bond (His C: 194), a carbon hydrogen bond bond (Thr C: 226), two bonds alkyl (Ala C: 135); (ile: 13), a pi-alkyl bond (Ala C: 198). It can be seen that the ligand Machilin G interacted with a large part of the main amino acids Ile13 (van der alkyl bond), Pro136, Thr197, Thr197 (van der halls), Cys166 (conventional hydrogen bond), His194 (pi-sigma)(Figure 6).

Table 3: Distances between the *TcGAPDH* residues and the ligands

***TcGAPDH* residue**	**Benznidazole**	**Chalepin (BRZ)**	**Machilin G**
Ile13	3.6 Å	5.4 Å	3.7
Pro136	5.5 Å	6.3 Å	4.9
Cys166	3.8 Å	1.2 Å	3.7
Thr167	4.1 Å	3.7 Å	3.2
His194	3.3 Å	3.2 Å	3.1
Thr197	5.0 Å	4.4 Å	3.4
Asp210	7.5 Å	3.7 Å	8.5
Arg249	5.0 Å	3.3 Å	5.7

ISSN- 2350-0530(O), ISSN- 2394-3629(P)
Index Copernicus Value (ICV 2018): 86.20
DOI: 10.5281/zenodo.3698202

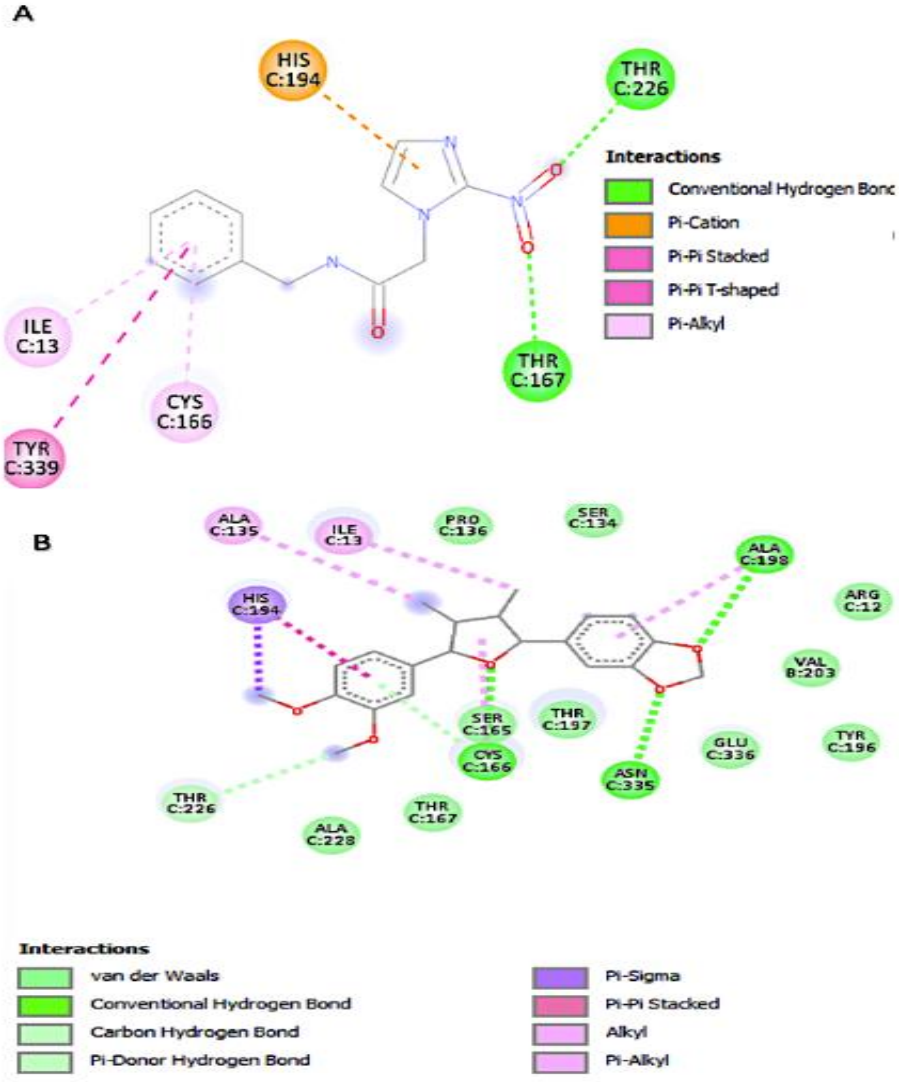

Figure 6: Two-dimensional molecular map for intermolecular interactions between *glyceraldehyde-3-phosphate dehydrogenase (TcGAPDH)* and Benznidazole (A), Machilin G (B)

3.7. Analysis of Molecular Docking Simulations Between *Trypanosoma Cruzi Tripanotiona Reductase (Tctr)* And Machilin G

The parasite, T. cruzi, has an essential enzyme called *Tripanothione reductase (TcTR)* a dimeric flavoprotein that belongs to the class of oxidoreductase enzymes, and is linked to the protection against oxidative stress of parasitic cells. performs the same cell protection function as human *Glutathione Reductase (GR), T. cruzi Trypanothione Reductase (TcTR)* allows the parasite to be unaffected by the defense mechanisms of the human host's immune system[27]. Biological and molecular genetic studies have shown that, in the absence of the *Tripanothione reductase-trypanothione* system, the parasite is more susceptible to oxidative stress, thus, it does not develop. One of the inhibitors used to work with this enzyme is quinacrine mustard, an alkylating derivative of the competitive inhibitor quinacrine that irreversibly inactivates *Tripanothione reductase*, but not human glutathione reductase. *T. cruzi* survival depends mainly on this enzyme. Therefore, the

ISSN- 2350-0530(O), ISSN- 2394-3629(P)
Index Copernicus Value (ICV 2018): 86.20
DOI: 10.5281/zenodo.3698202

search for molecules that are selective to *TcTR* constitutes a promising field for the planning of drugs against Chagas disease [53][54][55]. It presented an rmsd of 1507, and an affinity of -7.6 four alkyl bonds (Pro A: 336), two pi-sigma bonds (Ile A: 339), eight van der Waals interactions (Cys A: 53; Tyr A: 111; Thr A: 335; Asn A: 340; Glu A: 19; Arg A: 335; Ala A: 343; Asn A: 23). Interactions with the main residues of the type Glu19, Tyr111 (van der walls, and Ile339 (pi-sigma)) (Table 4) (Figure 7).

Table 4: Distances between the *Trypanosoma cruzi Tripanotiona Reductase (TcTR)* residues and the ligands

***Tripanotiona Reductase* residue**	**Benznidazole**	**Quinacrine Mustard (QUM)**	**Machilin G**
Ser15	13.4 Å	4.2 Å	4.9
Leu18	19.6 Å	3.2 Å	5.1
Glu19	18.1 Å	2.7 Å	3.5
Trp22	24.1 Å	3.5 Å	7.1
Ser110	26.4 Å	4.2 Å	9.9
Tyr111	19.5 Å	2.6 Å	4.0
Glu113	29.6 Å	1.5 Å	12.5
Met114	26.1 Å	3.3 Å	7.5
Asp117	33.0 Å	1.5 Å	14.7
Ile339	12.6 Å	3.5 Å	3.6

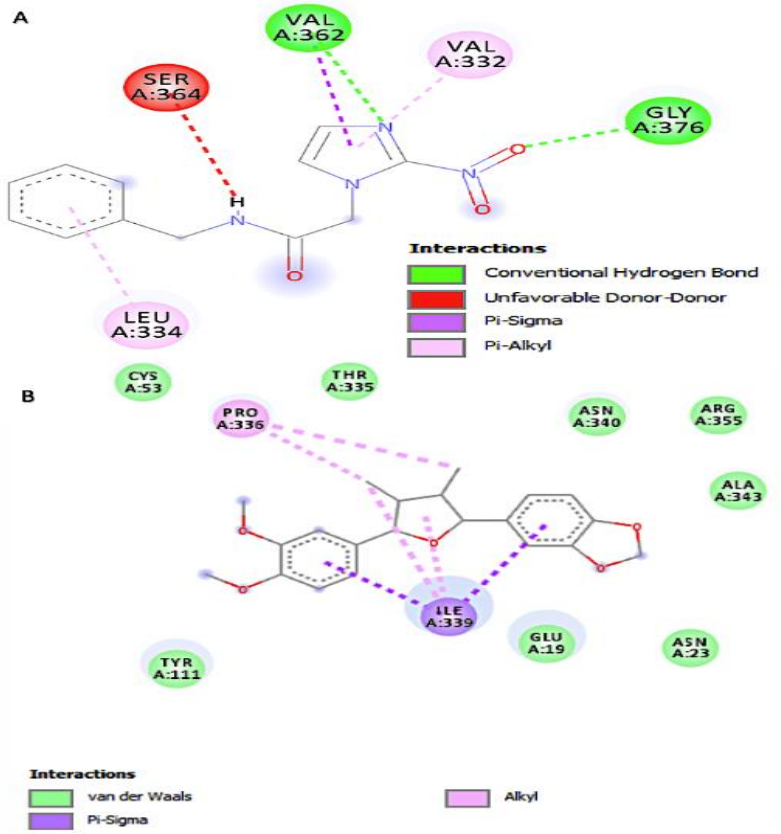

Fig. 7: Two-dimensional molecular map for intermolecular interactions *between Tripanothione Reductase (TcTR)* and Benznidazole (A), Machilin G (B)

ISSN- 2350-0530(O), ISSN- 2394-3629(P)
Index Copernicus Value (ICV 2018): 86.20
DOI: 10.5281/zenodo.3698202

4. Conclusions

Machilin G was geometrically optimized using semi-empirical quantum calculations, through this technique it was possible to generate the thermodynamically more stable conformation. Through the method of analysis of the computational simulations of molecular anchoring it showed that the ligand Machilin G coupled in the active site of the enzyme *TcGAPDH*, in distances close to chalepin. Regarding Cruzain, it is possible to highlight that the ligand Machilin G did not interact with the amino acids of the active site of the enzyme, being at a considerable distance compared to the ligand KB2. With respect to the enzyme trypanothione reductase, the ligand Machilin G had few interactions with the amino acids of the active site. The intermolecular interactions found for the complex formed and the values obtained from the distance of the enzyme residues, indicate that Machilin G has potential application as a new inhibitor of the *Trypanosoma cruzi TcGAPDH* enzyme.

5. Supplementary Material

Table S1: Atomic properties of Machilin G after optimization, disregarding hydrogen atoms

Atom	Element	Type	Valence	Partial Charge	X(Å)	Y(Å)	Z(Å)
1	C	Car	3	-0.016	-1.80290	-0.02160	-1.34470
2	C	Car	3	-0.052	-0.89900	-1.05320	-1.11990
3	C	Car	3	0.162	-1.87540	1.05070	-0.44860
4	C	Car	3	0.162	-1.03230	1.07610	0.67820
5	C	Car	3	-0.011	-0.11900	0.03840	0.89080
6	C	Car	3	-0.015	-0.05250	-1.02700	-0.00950
7	O	O3	2	-0.491	-1.17150	2.07440	1.64280
8	C	C3	4	0,079	-0.19790	3.09310	1.52580
9	O	O3	2	-0.491	-2.85020	2.03370	-0.61560
10	C	C3	4	0.079	-2.52380	2.96870	-1.62530
11	C	C3	4	0.087	0.95080	-2.12010	0.26520
12	C	C3	4	-0.008	0.45960	-3.20890	1.26280
13	C	C3	4	-0.008	1.22800	-4.46090	0.78370
14	C	C3	4	0.087	1,49380	-4,18110	-0,71980
15	O	O3	2	-0.364	1.32600	-2.77690	-0.95600
16	C	C3	4	-0.059	-1.05000	-3,37080	1.27680
17	C	C3	4	-0.059	0.53140	-5.78940	0.99730
18	C	Car	3	-0.015	2.87900	-4.63060	-1.12520
19	C	Car	3	-0.011	4.00050	-3.83900	-0.81630
20	C	Car	3	0.167	5.22530	-4.33820	-1.21200
21	C	Car	3	0.166	5.35360	-5.57180	-1.88020
22	C	Car	3	-0.016	4.25790	-6.35650	-2.18200
23	C	Car	3	-0.052	3.01070	-5.85240	-1.78750
24	O	O3	2	-0.453	6.48280	-3.76750	-1.03840
25	C	C3	4	0.233	7.42100	-4.68780	-1.63250
26	O	O3	2	-0.453	6.69460	-5.82100	-2.15170
27	H	H	1	0.066	-2.46220	-0.04910	-2.22020

ISSN- 2350-0530(O), ISSN- 2394-3629(P)
Index Copernicus Value (ICV 2018): 86.20
DOI: 10.5281/zenodo.3698202

28	H	H	1	0.062	-0.85460	-1.89420	-1.82270
29	H	H	1	0.066	0.54100	0.06390	1.76730
30	H	H	1	0.066	0.81780	2.70110	1.65320
31	H	H	1	0.066	-0.45050	3.76830	2.34650
32	H	H	1	0.066	-0.27190	3.61840	0.56590
33	H	H	1	0.066	-1.63060	3.54890	-1,36390
34	H	H	1	0.066	-3.40180	3.61830	-1.65040
35	H	H	1	0.066	-2.37720	2.48780	-2.59950
36	H	H	1	0.065	1.89280	-1.65420	0.64600
37	H	H	1	0.033	0.78310	-2.93640	2.29360
38	H	H	1	0.033	2.0660	-4.49360	1.32260
39	H	H	1	0.065	0.72470	-4.66330	-1.36830
40	H	H	1	0.023	-1.53950	-2,43380	1.57680
41	H	H	1	0.023	-1.36100	-4.14910	1,98620
42	H	H	1	0.023	-1.44090	-3.64230	0.28640
43	H	H	1	0.023	-0.43000	-5.84630	0.46780
44	H	H	1	0.023	0.33370	-5,96780	2.06210
45	H	H	1	0.023	1.15600	-6.61440	0,62850
46	H	H	1	0.066	3.89710	-2.87800	-0.30080
47	H	H	1	0.066	4.35020	-7.31430	-2.70140
48	H	H	1	0.062	2.11280	-6.44280	-2.00760
49	H	H	1	0.117	8.12390	-5.03430	-0.85890
50	H	H	1	0.117	7.94430	-4.18480	-2.46080

Table S2: Properties of Machilin G bonds after optimization, disregarding hydrogen atoms

Bond	**Type**	**Start Storm**	**End Storm**	**Bond Order**	**Rotable**	**Lenght(Å)**
1	C-C	C1	C2	2	No	1.38988
2	C-C	C1	C3	1	No	1.39931
3	C-H	C1	H1	1	No	1.09633
4	C-C	C2	C6	1	No	1.39651
5	C-H	C2	H2	1	No	1.0969
6	C-C	C3	C4	2	No	1.40753
7	C-O	C3	O2	1	No	1.39442
8	C-C	C4	C5	1	No	1.39862
9	C-O	C4	O1	1	No	1.39515
10	C-C	C5	C6	2	No	1.39644
11	C-H	C5	H3	1	No	1.0975
12	C-C	C6	C9	1	No	1.50895
13	O-C	O1	C7	1	No	1.41398
14	C-H	C7	H4	1	No	1.09615
15	C-H	C7	H5	1	No	1.09236
16	C-H	C7	H6	1	No	1.09673
17	O-C	O2	C8	1	No	1.4143
18	C-H	C8	H7	1	No	1.09671

ISSN- 2350-0530(O), ISSN- 2394-3629(P)
Index Copernicus Value (ICV 2018): 86.20
DOI: 10.5281/zenodo.3698202

19	C-H	C8	H8	1	No	1.09247
20	C-H	C8	H9	1	No	1.09628
21	C-C	C9	C10	1	Yes	1.55627
22	C-O	C9	O3	1	Yes	1.43649
23	C-H	C9	H10	1	No	1.11778
24	C-C	C10	C11	1	Yes	1.54515
25	C-C	C10	C13	1	No	1.51832
26	C-H	C10	H11	1	No	1.11421
27	C-C	C11	C12	1	Yes	1.55224
28	C-C	C11	C14	1	No	1.51519
29	C-H	C11	H12	1	No	1.11765
30	C-O	C12	O3	1	Yes	1.43378
31	C-C	C12	C15	1	No	1.51168
32	C-H	C12	H13	1	No	1.11561
33	C-H	C13	H14	1	No	1.0989
34	C-H	C13	H15	1	No	1.09805
35	C-H	C13	H16	1	No	1.09882
36	C-H	C14	H17	1	No	1.09904
37	C-H	C14	H18	1	No	1.09759
38	C-H	C14	H19	1	No	1.09853
39	C-C	C15	C16	2	No	1.40706
40	C-C	C15	C20	1	No	1.39599
41	C-C	C16	C17	1	No	1.38055
42	C-H	C16	H20	1	No	1.09542
43	C-C	C17	C18	2	No	1.4088
44	C-O	C17	O4	1	No	1.39181
45	C-C	C18	C19	1	No	1.38109
46	C-O	C18	O5	1	No	1.39072
47	C-C	C19	C20	2	No	1.40188
48	C-H	C19	H21	1	No	1.09347
49	C-H	C20	H22	1	No	1.09692
50	O-C	O4	C21	1	No	1.44226
51	C-O	C21	O5	1	No	1.44269
52	C-H	C21	H23	1	No	1.10118
53	C-H	C21	H24	1	no	1.10133

Table S3: Angle properties of Machilin G after optimization, disregarding hydrogen atoms

Angle	Type	Start Atom	Vertex	End Atom	Angle (°)
1	CCC	C2	C1	C3	119.9264
2	CCH	C2	C1	H1	120.1087
3	CCH	C3	C1	H1	119.9643
4	CCC	C1	C2	C6	120.5898

ISSN- 2350-0530(O), ISSN- 2394-3629(P)
Index Copernicus Value (ICV 2018): 86.20
DOI: 10.5281/zenodo.3698202

5	CCH	C1	C2	H2	119.4565
6	CCH	C6	C2	H2	119.9536
7	CCC	C1	C3	C4	119.6998
8	CCO	C1	C3	O2	119.9823
9	CCO	C4	C3	O2	120.1253
10	CCC	C3	C4	C5	119.9632
11	CCO	C3	C4	O1	120.4408
12	CCO	C5	C4	O1	119.4035
13	CCC	C4	C5	C6	119.9442
14	CCH	C4	C5	H3	119.7920
15	CCH	C6	C5	H3	120.2635
16	CCC	C2	C6	C5	119.8727
17	CCC	C2	C6	C9	122.2890
18	CCC	C5	C6	C9	117.8383
19	COC	C4	O1	C7	112.9302
20	OCH	O1	C7	H4	111.7624
21	OCH	O1	C7	H5	102.9398
22	OCH	O1	C7	H6	111.7794
23	HCH	H4	C7	H5	110.3648
24	HCH	H4	C7	H6	109.6049
25	HCH	H5	C7	H6	110.2376
26	COC	C3	O2	C8	112.9677
27	OCH	O2	C8	H7	111.5643
28	OCH	O2	C8	H8	102.9456
29	OCH	O2	C8	H9	112.0416
30	HCH	H7	C8	H8	110.2093
31	HCH	H7	C8	H9	109.5706
32	HCH	H8	C8	H9	110.3585
33	CCC	C6	C9	C10	114.4343
34	CCO	C6	C9	O3	110.4948
35	CCH	C6	C9	H10	108.6881
36	CCO	C10	C9	O3	107.9089
37	CCH	C10	C9	H10	109.8294
38	OCH	O3	C9	H10	105.0746
39	CCC	C9	C10	C11	102.1908
40	CCC	C9	C10	C13	113.2239
41	CCH	C9	C10	H11	109.2864
42	CCC	C11	C10	C13	114.2614
43	CCH	C11	C10	H11	109.9158
44	CCH	C13	C10	H11	107.8317
45	CCC	C10	C11	C12	103.8529
46	CCC	C10	C11	C14	115.9829
47	CCH	C10	C11	H12	108.0369
48	CCC	C12	C11	C14	111.9204

ISSN- 2350-0530(O), ISSN- 2394-3629(P)
Index Copernicus Value (ICV 2018): 86.20
DOI: 10.5281/zenodo.3698202

49	CCH	C12	C11	H12	108.8065
50	CCH	C12	C11	H12	107.9942
51	CCO	C11	C12	O3	108.4250
52	CCC	C11	C12	C15	111.2887
53	CCH	C11	C12	H13	111.5358
54	OCC	O3	C12	C15	110.7492
55	OCH	O3	C12	H13	104.2922
56	CCH	C15	C12	H13	110.3224
57	COC	C9	O3	C12	109.7741
58	CCH	C10	C13	H14	110.7618
59	CCH	C10	C13	H15	111.2931
60	CCH	C10	C13	H16	111.8228
61	HCH	H14	C13	H15	107.5680
62	HCH	H14	C13	H16	107.3543
63	HCH	H15	C13	H16	107.3543
64	CCH	C11	C14	H17	112.3115
65	CCH	C11	C14	H18	112.3115
66	CCH	C11	C14	H19	107.8206
67	HCH	H17	C14	H18	107.5423
68	HCH	H17	C14	H19	107.2622
69	HCH	H18	C14	H19	107.8206
70	CCC	C12	C15	C16	120.2784
71	CCC	C12	C15	C20	118.2896
72	CCC	C16	C15	C20	121.4230
73	CCC	C15	C16	C17	116.1535
74	CCH	C15	C16	H20	121.4417
75	CCH	C17	C16	H20	122.4016
76	CCC	C16	C17	C18	122.2335
77	CCO	C16	C17	O4	128.1374
78	CCO	C18	C17	O4	109.6288
79	CCC	C17	C18	C19	121.9320
80	CCO	C17	C18	O5	109.7133
81	CCO	C19	C18	O5	128.3547
82	CCC	C18	C19	C20	116.1053
83	CCH	C18	C19	H21	122.3109
84	CCH	C20	C19	H21	121.5835
85	CCC	C15	C20	C19	122.1517
86	CCH	C15	C20	H22	119.2778
87	CCH	C19	C20	H22	118.5704
88	COC	C17	O4	C21	105.9445
89	OCO	O4	C21	O5	108.7790
90	OCH	O4	C21	H23	109.0643
91	OCH	O4	C21	H24	109.1147

ISSN- 2350-0530(O), ISSN- 2394-3629(P)
Index Copernicus Value (ICV 2018): 86.20
DOI: 10.5281/zenodo.3698202

92	OCH	O5	C21	H23	109.0904
93	OCH	O5	C21	H24	109.1061
94	HCH	H23	C21	H24	111.6400
95	COC	C18	O5	C21	105.9321

Table S4: Torsional properties of Machilin G after optimization, disregarding hydrogen atoms

Torsion	Type	Atom 1	Atom 2	Atom 3	Atom 4	Torsion (°)
1	CCCC	C3	C1	C2	C6	-0.4244
2	CCCH	C3	C1	C2	H2	179.4829
3	HCCC	H1	C1	C2	C6	179.8629
4	HCCH	H1	C1	C2	H2	-0.2298
5	CCCC	C2	C1	C3	C4	-0.1191
6	CCCO	C2	C1	C3	O2	-175.0833
7	HCCC	H1	C1	C3	C4	179.5940
8	HCCO	H1	C1	C3	O2	4.6298
9	CCCC	C1	C2	C6	C5	0.4950
10	CCCC	C1	C2	C6	C9	-179.4713
11	HCCC	H2	C2	C6	C5	-179.4118
12	HCCC	H2	C2	C6	C9	0.6219
13	CCCC	C1	C3	C4	C5	0.5907
14	CCCO	C1	C3	C4	O1	-174.3365
15	OCCC	O2	C3	C4	C5	175.5476
16	OCCO	O2	C3	C4	O1	0.6204
17	CCOC	C1	C3	O2	C8	-78.6072
18	CCOC	C4	C3	O2	C8	106.4503
19	CCCC	C3	C4	C5	C6	-0.5215
20	CCCH	C3	C4	C5	H3	179.6546
21	OCCC	O1	C4	C5	C6	174.4584
22	OCCH	O1	C4	C5	H3	-5.3654
23	CCOC	C3	C4	O1	C7	-101.7578
24	CCOC	C5	C4	O1	C7	83.2867
25	CCCC	C4	C5	C6	C2	-0.0184
26	CCCC	C4	C5	C6	C9	179.9495
27	HCCC	H3	C5	C6	C2	179.8046
28	HCCC	H3	C5	C6	C9	-0.2275
29	CCCC	C2	C6	C9	C10	-96.2868
30	CCCO	C2	C6	C9	O3	25.7459
31	CCCH	C2	C6	C9	H10	140.5512
32	CCCC	C5	C6	C9	C10	83.7462
33	CCCO	C5	C6	C9	O3	-154.2211
34	CCCH	C5	C6	C9	H10	-39.4158
35	COCH	C4	O1	C7	H4	-61.1714
36	COCH	C4	O1	C7	H5	-179.6082
37	COCH	C4	O1	C7	H6	62.0967

ISSN- 2350-0530(O), ISSN- 2394-3629(P)
Index Copernicus Value (ICV 2018): 86.20
DOI: 10.5281/zenodo.3698202

38	COCH	C3	O2	C8	H7	-64.5199
39	COCH	C3	O2	C8	H8	177.3169
40	COCH	C3	O2	C8	H9	58.7503
41	CCCC	C6	C9	C10	C11	150.4081
42	CCCC	C6	C9	C10	C13	27.0308
43	CCCH	C6	C9	C10	H11	-93.1803
44	OCCC	O3	C9	C10	C11	26.9742
45	OCCC	O3	C9	C10	C13	-96.4031
46	OCCH	O3	C9	C10	H11	143.3858
47	HCCC	H10	C9	C10	C11	-87.0473
48	HCCC	H10	C9	C10	C13	149.5754
49	HCCH	H10	C9	C10	H11	29.3643
50	CCOC	C6	C9	O3	C12	-142.4469
51	CCOC	C10	C9	O3	C12	-16.6523
52	HCOC	H10	C9	O3	C12	100.4924
53	CCCC	C9	C10	C11	C12	-26.1870
54	CCCC	C9	C10	C11	C14	-149.4114
55	CCCH	C9	C10	C11	H12	89.2484
56	CCCC	C13	C10	C11	C12	96.4882
57	CCCC	C13	C10	C11	C14	-26.7362
58	CCCH	C13	C10	C11	H12	-148.0763
59	HCCC	H11	C10	C11	C12	-142.1428
60	HCCC	H11	C10	C11	C14	94.6328
61	HCCH	H11	C10	C11	H12	-26.7074
62	CCCH	C9	C10	C13	H14	-60.6837
63	CCCH	C9	C10	C13	H15	59.0139
64	CCCH	C9	C10	C13	H16	59.0139
65	CCCH	C11	C10	C13	H14	-177.1356
66	CCCH	C11	C10	C13	H15	-57.4379
67	CCCH	C11	C10	C13	H16	-57.4379
68	HCCH	H11	C10	C13	H14	60.3525
69	HCCH	H11	C10	C13	H15	-59.2647
70	HCCH	H11	C10	C13	H16	-179.9499
71	CCCO	C10	C11	C12	O3	17.9398
72	CCCC	C10	C11	C12	C15	139.9844
73	CCCH	C10	C11	C12	H13	-96.3406
74	CCCO	C14	C11	C12	O3	143.7871
75	CCCC	C14	C11	C12	C15	-94.1684
76	CCCH	C14	C11	C12	H13	29.5067
77	HCCO	H12	C11	C12	O3	-96.9499
78	HCCC	H12	C11	C12	C15	25.0946
79	HCCH	H12	C11	C12	H13	148.7697
80	CCCH	C10	C11	C14	H17	148.7697
81	CCCH	C10	C11	C14	H18	112.3192

ISSN- 2350-0530(O), ISSN- 2394-3629(P)
Index Copernicus Value (ICV 2018): 86.20
DOI: 10.5281/zenodo.3698202

82	CCCH	C10	C11	C14	H19	-115.3737
83	CCCH	C12	C11	C14	H17	-118.8964
84	CCCH	C12	C11	C14	H18	-6.1431
85	CCCH	C12	C11	C14	H19	125.7299
86	HCCH	H12	C11	C14	H17	121.3630
87	HCCH	H12	C11	C14	H18	-126.3233
88	HCCH	H12	C11	C14	H19	5.9893
89	CCOC	C11	C12	O3	C9	-0.9488
90	CCOC	C15	C12	O3	C9	-123.3223
91	HCOC	H13	C12	O3	C9	118.0075
92	CCCC	C11	C12	C15	C16	-78.6900
93	CCCC	C11	C12	C15	C20	100.2399
94	OCCC	O3	C12	C15	C16	41.9977
95	OCCC	O3	C12	C15	C20	-139.0723
96	HCCC	H13	C12	C15	C16	156.9475
97	HCCC	H13	C12	C15	C20	-24.1226
98	CCCC	C12	C15	C16	C17	179.2402
99	CCCH	C12	C15	C16	H20	-1.3959
100	CCCC	C20	C15	C16	C17	0.3444
101	CCCH	C20	C15	C16	H20	179.7083
102	CCCC	C12	C15	C20	C19	-179.0204
103	CCCH	C12	C16	C20	H22	0.8634
104	CCCC	C16	C16	C20	C19	-0.1033
105	CCCH	C16	C16	C20	H22	179.7805
106	CCCC	C15	C16	C17	C18	-0.3480
107	CCCO	C15	C16	C17	O4	179.8891
108	HCCC	H20	C16	C17	C18	-179.7052
109	HCCO	H20	C16	C17	O4	0.5319
110	CCCC	C16	C17	C18	C19	0.1087
111	CCCO	C16	C17	C18	O5	-179.8470
112	OCCC	O4	C17	C18	C19	179.9106
113	OCCO	O4	C17	C18	O5	-0.0450
114	CCOC	C16	C17	O4	C21	-179.8896
115	CCOC	C18	C17	O4	C21	0.3233
116	CCCC	C17	C18	C19	C20	0.1452
117	CCCH	C17	C18	C19	H21	179.9260
118	OCCC	O5	C18	C19	C20	-179.9080
119	OCCH	O5	C18	C19	H21	-0.1272
120	CCOC	C17	C18	O5	C21	-0.2534
121	CCOC	C19	C18	O5	C21	179.7946
122	CCCC	C18	C19	C20	C15	-0.1462
123	CCCH	C18	C19	C20	H22	179.9692
124	HCCC	H21	C19	C20	C15	-179.9287
125	HCCH	H21	C19	C20	H22	0.1868

ISSN- 2350-0530(O), ISSN- 2394-3629(P)
Index Copernicus Value (ICV 2018): 86.20
DOI: 10.5281/zenodo.3698202

126	COCO	C17	O4	C21	O5	-0.4796
127	COCH	C17	O4	C21	H23	-119.3612
128	COCH	C17	O4	C21	H24	118.4501
129	OCOC	O4	C21	O5	C18	0.4531
130	HCOC	H23	C21	O5	C18	119.3183
131	HCOC	H24	C21	O5	C18	-118.4820

Acknowledgements

The present work was partially funded by CNPq - National Council for Scientific and Technological Development and CAPES - Brazilian Federal Agency for Support and Evaluation of Postgraduate Education of the Brazilian Ministry of Education.

References

[1] N. Grandisin et al., "Antileishmanial Activity and Structure-Activity Relationship of Triazolic Compounds Derived from the Neolignans Grandisin, Veraguensin, and Machilin G," no. Cl, 2016.
[2] T. B. Cassamale, E. C. Costa, D. B. Carvalho, and N. S. Cassemiro, "Tatiana B. Cassamale," vol. 27, no. 7, pp. 1217–1228, 2016.
[3] G. E. Miana, S. R. Ribone, D. M. A. Vera, S. Manuel, M. R. Mazzieri, and M. A. Quevedo, "European Journal of Medicinal Chemistry Design , synthesis and molecular docking studies of novel N -arylsulfonyl-benzimidazoles with anti Trypanosoma cruzi activity," vol. 165, pp. 1–10, 2019.
[4] "Universidade federal da bahia faculdade de medicina fundação oswaldo cruz," 2017.
[5] M. M. Marinho et al., "Molecular Fractionation With Conjugate Caps Study Of The Interaction Of The Anacardic Acid With The Active Site Of Trypanosoma Cruzi Gapdh Enzyme : A Quantum Investigation," Asian J Pharm Clin Res, vol. 12, no. 12, 2019.
[6] F. F. Ribeiro, F. J. B. M. Junior, M. S. da Silva, M. T. ulliu. Scotti, and L. Scotti, "Computational and Investigative Study of Flavonoids Active Against Typanosoma cruzi and Leishmania spp," Nat. Prod. Commun., 2015.
[7] T. B. Cassamale et al., "Synthesis and Antitrypanosomastid Activity of 1,4-Diaryl-1,2,3-triazole Analogues of Neolignans Veraguensin, Grandisin and Machilin G," J. Braz. Chem. Soc., 2016.
[8] A. R. das Neves et al., "Effect of isoxazole derivatives of tetrahydrofuran neolignans on intracellular amastigotes of Leishmania (Leishmania) amazonensis: A structure–activity relationship comparative study with triazole-neolignan-based compounds," Chem. Biol. Drug Des., 2019.
[9] O. S. Trefzger et al., "Design, synthesis and antitrypanosomatid activities of 3,5-diaryl-isoxazole analogues based on neolignans veraguensin, grandisin and machilin G," Chem. Biol. Drug Des., 2019.
[10] E. J. Braga, B. T. Corpe, M. M. Marinho, and E. S. Marinho, "Molecular electrostatic potential surface, HOMO–LUMO, and computational analysis of synthetic drug Rilpivirine," Int. J. Sci. Eng. Res., vol. 7, no. 7, pp. 315–319, 2016.
[11] M. Reges, M. M. Marinho, and E. S. Marinho, "Semi-Empirical Study of the Drug Riociguat , an Important Drug for Oral Treatment against Chronic Thromboembolic Pulmonary Hypertension," Int. J. Sci. Eng. Sci., vol. 1, no. 1, pp. 13–17, 2017.
[12] E. S. Marinho and M. M. Marinho, "A DFT study of synthetic drug topiroxostat: MEP, HOMO, LUMO," Int. J. Sci. Eng. Res., vol. 7, no. July, pp. 1264–1270, 2016.

ISSN- 2350-0530(O), ISSN- 2394-3629(P)
Index Copernicus Value (ICV 2018): 86.20
DOI: 10.5281/zenodo.3698202

[13] J. Silva, A. R. Lima, L. L. Bezerra, M. M. Marinho, and E. S. Marinho, "Bixinoids potentially active against dengue virus: a molecular docking study," JInternational J. Sci. Eng. Res., vol. 8, no. 4, pp. 882–887, 2017.
[14] A. R. Lima, J. Silva, L. L. Bezerra, M. M. Marinho, and E. S. Marinho, "Molecular docking of potential curcuminoids inhibitors of the NS1 protein of dengue virus," Int. J. Sci. Eng. Res., vol. 8, no. 4, 2017.
[15] E. S. M. G. A. Araújo, E. P. Silva, E. P. Sanabio, J. A. Pinheiro, R.R. Castro, R.R. Castro, M.M. Marinho, F. K. S.Lima, "Characterization in Silico of the Structural Parameters of the Antifungal Agent Ketoconazole," Sci. Signpost Publ., 2016.
[16] M. Reges, M. M. Marinho, and E. S. Marinho, "In Silico Characterization of Hypoglycemic Agent Phenformin Using Classical Force Field MMFF94," Int. J. Recent Res. Rev., vol. XI, no. 2, pp. 36–43, 2018.
[17] J. Silva, A. R. Lima, L. L. Bezerra, M. M. Marinho, and E. S. Marinho, "Molecular coupling study between the potential inhibitor of dengue fever, Annatto and Protein E (DENV-4)," Int. J. Sci. Eng. Res. Vol., vol. 8, no. 7, pp. 815–821, 2017.
[18] M. M. Marinho, R. R. Castro, and E. S. Marinho, "Utilização Do Método Semi-Empírico Pm7 Para Caracterização Do Fármaco Atalureno : Homo ,Lumo, Mesp," Rev. Expressão Católica, vol. 1, no. 1, pp. 177–184, 2016.
[19] Protein Data Bank, "RCSB PDB: Homepage," RCSB PDB, 2019. .
[20] S. Kim et al., "PubChem 2019 update: Improved access to chemical data," Nucleic Acids Res., 2019.
[21] J. Mancuso and R. J. McEachern, "Applications of the PM3 semi-empirical method to the study of triethylenediamine," J. Mol. Graph. Model., 1997.
[22] S. S. Carneiro, M. M. Marinho, and E. S. Marinho, "Electronic / Structural Characterization of Antiparkinsonian Drug Istradefylline : A Semi-Empirical Study," Int. J. Recent Res. Rev., vol. X, no. 4, pp. 9–14, 2017.
[23] V. M. De Oliveira, M. M. Marinho, and E. S. Marinho, "Semi-Empirical Quantum Characterization of the Drug Selexipag : HOMO and LUMO and Reactivity Descriptors," Int. J. Recent Res. Rev., vol. XII, no. 2, pp. 15–20, 2019.
[24] A. R. Lima, E. M. Marinho, J. Silva, M. M. Marinho, and E. S. Marinho, "Estudo In Silico Do Flavonoide Antitrombótico Ternatina , Presente Nos Capítulos Florais De In Silico Study Of Flavonoid Antithrombotic Ternatin Present In The Flowers Chapters Of Egletes Viscosa Less ' Macela -Da- Terra ,'" Rev. Expressão Católica Saúde, vol. 2, no. 1, 2017.
[25] K. Brak et al., "Nonpeptidic tetrafluorophenoxymethyl ketone Cruzain inhibitors as promising new leads for chagas disease chemotherapy," J. Med. Chem., 2010.
[26] F. Pavão et al., "Structure of Trypanosoma cruzi glycosomal glyceraldehyde-3-phosphate dehydrogenase complexed with chalepin, a natural product inhibitor, at 1.95 AÅ resolution," FEBS Lett., 2002.
[27] A. Saravanamuthu, T. J. Vickers, C. S. Bond, M. R. Peterson, W. N. Hunter, and A. H. Fairlamb, "Two interacting binding sites for quinacrine derivatives in the active site of trypanothione reductase: A template for drug design," J. Biol. Chem., 2004.
[28] F. N. M. Lucio, J. E. da Silva, E. M. Marinho, F. R. D. S. Mendes, M. M. Marinho, and E. S. Marinho, "Methylcytisine Alcaloid Potentially Active Against Dengue Virus : A Molecular Docking Study And Electronic Structural Characterization," Int. J. Res. -GRANTHAALAYAH, vol. 8, no. January, pp. 221–236, 2020.
[29] A. K. Agrahari and C. George Priya Doss, "A Computational Approach to Identify a Potential Alternative Drug With Its Positive Impact Toward PMP22," J. Cell. Biochem., 2017.
[30] R. Huey, G. M. Morris, and S. Forli, "Using autodock 4 and autodock vina with autodocktools : a tutorial," 2012.

ISSN- 2350-0530(O), ISSN- 2394-3629(P)
Index Copernicus Value (ICV 2018): 86.20
DOI: 10.5281/zenodo.3698202

[31] D. S. BIOVIA et al., "Dassault Systèmes BIOVIA, Discovery Studio Visualizer, v.17.2, San Diego: Dassault Systèmes, 2016. ," J. Chem. Phys., 2000.
[32] E. F. Pettersen et al., "UCSF Chimera - A visualization system for exploratory research and analysis," J. Comput. Chem., vol. 25, no. 13, pp. 1605–1612, 2004.
[33] A. Arroio, K. M. Honório, and A. B. F. Da Silva, "Propriedades químico-quânticas empregadas em estudos das relações estrutura-atividade," Quim. Nova, vol. 33, no. 3, pp. 694–699, 2010.
[34] B. Nagy and F. Jensen, "Basis Sets in Quantum Chemistry," 2017.
[35] D. Lopes et al., "Characterization of the natural pesticide 6-desoxyclitoriacetal: a quantum study," Int. J. Sci. Eng. Res., 2019.
[36] L. Paes, W. L. Santos, M. M. Marinho, and E. S. Marinho, "Estudo Dft Do Alcaloide Dicentrina: Gap, Homo, Lumo, Mesp E Mulliken," JOIN, no. 1, 2017.
[37] T. Koopmans, "Über die Zuordnung von Wellenfunktionen und Eigenwerten zu den Einzelnen Elektronen Eines Atoms," Physica, 1934.
[38] F. Jensen, "Atomic orbital basis sets," Wiley Interdisciplinary Reviews: Computational Molecular Science. 2013.
[39] F. Jensen, "The optimum contraction of basis sets for calculating spin-spin coupling constants," Theor. Chem. Acc., 2010.
[40] "Cargas Atômicas em Moléculas," Quim. Nova, 1996.
[41] N. Prabavathi, A. Nilufer, and V. Krishnakumar, "Molecular structure, vibrational, UV, NMR, hyperpolarizability, NBO and HOMO-LUMO analysis of Pteridine2,4-dione," Spectrochim. Acta - Part A Mol. Biomol. Spectrosc., 2012.
[42] P. T. Okoli et al., "In Silico Study of Phytochemical Chlorogenic Acid : A Semi- Empirical Quantum Study and Adme," Int. J. Recent Res. Rev., vol. 52, no. 4, pp. 345–357, 2019.
[43] Kotz, Chemistry & Chemical Reactivity. 2014.
[44] C. Henrique et al., "Characterization of the natural insecticide methylcytisine: An in silico study using classic force field," Int. J. Recent Res. Rev., vol. XII, no. 2, pp. 15–20, 2019.
[45] D. Lopes et al., "In Silico Studies Of Sophoraflavanone G: Quantum Characterization And Admet," Int. J. Res. - GRANTHAALAYAH, vol. 7, no. November, pp. 160–179, 2019.
[46] R. B. de A. E. J. Barreiro, C. R. Rodrigues, M. G. Albuquerque, C. M. R. de Sant'anna, "Molecular Modeling: A Tool for the Rational Planning of Drugs in Medicinal Chemistry," New Chem., vol. 20, p. 1, 1997.
[47] E. J. Barreiro, C. Alberto, and M. Fraga, Química medicinal: as bases moleculares da ação dos fármacos. .
[48] A. R. Lima and E. S. Marinho, "Alicina uma potencial aliada contra a Chikungunya (CHIKV): um estudo de docking molecular," An. do XXIII Encontro Iniciac. a Pesqui. -UNIFOR, vol. 3, 2017.
[49] J. C. Kotz, P. M. Treichel, and J. R. Townsend, Chemistry and Chemical Reactivity. 2012.
[50] D. Yusuf, A. M. Davis, G. J. Kleywegt, and S. Schmitt, "An alternative method for the evaluation of docking performance: RSR vs RMSD," J. Chem. Inf. Model., 2008.
[51] R. A. Costa et al., "CHEMISTRY Studies of NMR , molecular docking , and molecular dynamics simulation of new promising inhibitors of Cruzaine from the parasite Trypanosoma cruzi," Med. Chem. Res., pp. 246–259, 2019.
[52] A. A. De Marchi, S. Castilho, P. Gustavo, B. Nascimento, C. Archanjo, and D. Ponte, "New 3-piperonylcoumarins as inhibitors of glycosomal glyceraldehyde-3-phosphate dehydrogenase (gGAPDH) from Trypanosoma cruzi," vol. 12, pp. 4823–4833, 2004.
[53] A. Saravanamuthu et al., "Enzyme Catalysis and Regulation : Two Interacting Binding Sites for Quinacrine Derivatives in the Active Site of Trypanothione Reductase : A TEMPLATE FOR DRUG DESIGN Two Interacting Binding Sites for Quinacrine Derivatives in the Active Site of Trypanothione Reductase," 2004.

ISSN- 2350-0530(O), ISSN- 2394-3629(P)
Index Copernicus Value (ICV 2018): 86.20
DOI: 10.5281/zenodo.3698202

[54] V. Screening, T. Reductase, and N. P. Database, "Artigo Triagem Virtual Aplicada na Busca de Inibidores da Tripanotiona Redutase de Trypanosoma cruzi Utilizando a Base de Dados de Produtos Naturais do Semiárido Baiano (NatProDB) Virtual Screening applied to search of inhibitors of Trypanosoma cruzi Trypanothione Reductase employing the Natural Products Database from Bahia state (NatProDB) Revista Virtual de Química Triagem Virtual Aplicada na Busca de Inibidores da Tripanotiona Redutase de Trypanosoma cruzi Utilizando a Base de Dados de Produtos Naturais do Semiárido Baiano (NatProDB) Vinícius G . da Paixão ,* Samuel S . R . Pita," vol. XX, no. Xx, 2016.

[55] S. S. R, S. S. R. Pita, and P. G. Pascutti, "Artigo Alvos Terapêuticos na Doença de Chagas : a Tripanotiona Redutase como Foco Therapeutic T argets in Chagas ' Disease : a Focus on Trypanothione Reductase Resumo Alvos Terapêuticos na Doença de Chagas : a Tripanotiona Redutase como Foco 1 . Panorama Global das Doenças," vol. 3, no. 4, pp. 307–324, 2011.

*Corresponding author.
E-mail address: emmanuel.marinho@ uece.br